Materials Research Express

PAPER

Influence of microballoon wall thickness on dynamic mechanical analysis of closed cell foams

To cite this article: Mrityunjay Doddamani 2019 *Mater. Res. Express* **6** 125348

Materials Research Express

PAPER

Influence of microballoon wall thickness on dynamic mechanical analysis of closed cell foams

RECEIVED
25 September 2019

REVISED
29 November 2019

ACCEPTED FOR PUBLICATION
17 December 2019

PUBLISHED
8 January 2020

Mrityunjay Doddamani

Lightweight Materials Laboratory, Department of Mechanical Engineering, National Institute of Technology Karnataka, Surathkal, 575025, India

E-mail: mrdoddamani@nitk.edu.in

Keywords: closed cell foam, glass microballoon, HDPE, wall thickness, DMA

Abstract

Thermoplastics are most commonly used in industrial and consumer products. The growing interest in making them lightweight is always a priority in industrial practices. Investigations on thermoplastic based closed cell foams wall thickness variations for dynamic mechanical analysis (DMA), and crystallinity are scarce. The present study investigates storage modulus, loss modulus, damping, and % crystallinity as a function of glass microballoon/high-density polyethylene (GMB/HDPE) foam wall thickness and volume fraction variations. Crystallinity percentage variation in HDPE and their foams are analyzed through DSC traces. GMBs are mixed with HDPE in plasticorder, and subsequently, GMB/HDPE composite blend is compression molded. Varying wall thickness (particle density variations) GMB particles across three different volume fractions (20, 40 and 60%) are prepared. Storage modulus, loss modulus, and damping are observed to be increasing with particle wall thickness and volume fraction as compared to HDPE matrix resin. Thick walled GMB particle with the highest GMB content registered enhanced storage modulus compared to thin walled ones at lower temperatures. DMA properties increase with increasing wall thickness. Damping is noted to be less sensitive than the storage and loss modulus. Crystallinity is observed to be decreasing with increasing wall thickness and GMB content. Higher crystalline phase contributes towards DMA properties at lower filler loadings while higher wall thickness plays a vital role at higher filler content.

Introduction

Closed cell foams are realized by embedding hollow microspheres in the matrix resin. The hollow structure of microballoons makes them closed cell foams [1]. These hollow microballoons permit to tailor-make the properties across two configurations namely wall thickness and volume fraction variations, and hence, they offer flexibility in designing materials for a wide range of applications. This feature makes them more attractive and noteworthy [2]. Further, these closed cell foams also offer superior mechanical properties coupled with moisture absorption [3] and find their application in buoyancy modules for submarine components [4, 5]. Favorable properties and lightweightness make them most suitable and sought after material in aerospace and marine sectors [6]. These closed cell foams are also widely used as a core in sandwiches owing to their better compressive strength and higher stiffness [7]. Hollow microballoons that define foam behavior are available in the spherical form of carbon, glass, fly ash cenospheres, expandable polymers, and ceramics [8–13]. The design and development of lightweight materials for weight-sensitive structures is changed since glass microballoons (GMBs) are manufactured in the 1960s [2]. Development of thermoplastic foams for sports, electronics, transportation, leisure and aerospace is always on priority by polymer industries. Engineered GMBs can be effectively embedded in thermoplastics and is a potential inexpensive candidate constituent with better mechanical properties like dimensional stability, lower dielectric constant, reduced thermal conductivity, heat distortion resistance and higher modulus [14, 15]. In comparison with other microballoons GMBs are inorganic

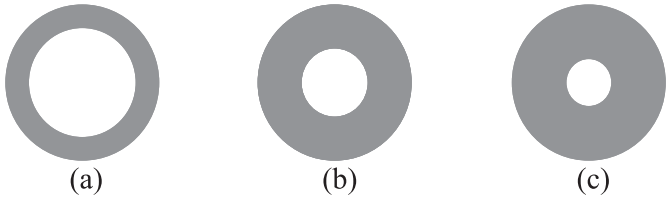

Figure 1. Schematic representation of (a) 200 (b) 270 and (c) 350 Kg m^{-3} density particles.

and more versatile [16–18]. Compression molding machines can exploit these GMB benefits if infused in compliant thermoplastics in developing lightweight components for weight sensitive applications.

Closed cell foams are widely investigated in the recent past [19–21]. Enhancement in storage and loss modulus is observed by Zeltmann *et al* [22] with fly ash cenospheres addition in thermoplastics. Thermally stable foam is realized with 5 °C enhancement in threshold storage modulus as compared to matrix. Increasing temperature increases damping. Microballoons addition results in 14%–66% lower damping compared to resin exhibiting post T_g higher storage moduli [23]. Improvement in loss and storage moduli until 30 weight % of the cenosphere is reported by Das and Satapathy [24]. Further, they noted increasing storage modulus with filler content at sub-zero temperatures. Nonetheless, such an enhancement is absent at elevated temperatures. GMB content addition is not directly proportional to storage moduli, as reported by Tagliavia *et al* [25]. GMB wall thickness effect in thermosetting resin is explored by Lin *et al* [26], wherein they noted that filler loading is less sensitive to thermal stability. Damping enhancement with filler addition is observed by Gu *et al* [27], attributing to higher frictional damping and the hollow structure of microballoons. Temperature rise decreases storage modulus [28]. Thermoplastics being reusable, mouldable, and recyclable are most preferred for engineering and semi-structural applications. Automotive parts, Jerry can cap, end caps for closure, square base attachment for pipes, and storage bins are made from the most widely consumed HDPE [29, 30]. Imbibing relatively inexpensive GMBs in HDPE resin through compression molding might lower thermoplastic consumption in addition to exhibiting better DMA properties and hence needs to be addressed to widen their possible structural and engineering applications.

The thermal transition of polymer materials is primarily characterized using DMA. Constituents interfacial bonding, blend miscibility, and associated properties are analyzed using the DMA technique [31–40]. The utility of this technique is explored further in recent investigations for heterogeneous materials as well [41–43]. Storage and loss moduli are correlated to the microstructure of the material in these studies. Nonetheless, comprehensive DMA investigations on the influence of wall thickness in closed cell thermoplastic foams developed through compression molding are not available in the literature. In the present study, GMBs are dispersed in HDPE using a compression molding route. Both the constituents are used in as-received condition. DMA properties are investigated in temperature sweep mode, and the influence of GMB wall thickness and volume fraction is analyzed for damping, storage, and loss modulus. Further, crystallinity studies are carried out to correlate with DMA properties.

Materials and methods

GMBs as hollow fillers of grades SID200, SID270, and SID350 in as received condition having average diameters of 53, 50, and 45 μm and the corresponding wall thickness of 0.716, 0.925, 1.080 μm are procured from Trelleborg Offshore, USA. These different density particles (200, 270, and 350 kg m^{-3}) are dispersed in the HDPE matrix (180M50 grade) supplied by IOCL, India, in ~3 mm dia. granular form. It has MFI (190 °C and 2.16 Kg), density (23 °C), tensile yield strength, elongation at yield, flexural modulus, shore D hardness and Vicat softening point (10 N) respectively of 20 g m/ 10 min (ASTM D1238), 950 Kg m^{-3} (ASTM D1505), 22 MPa (ASTM D638), 12% (ASTM D638), 750 MPa (ASTM D790), 55 (ASTM D2240) and 124 °C (ASTM D1525). Plasticoder is used for blending GMBs and HDPE matrix and are subsequently compression molded to form sheets. Processing details are available in [44]. HYYY-ZZ convention is used for naming the samples (H: HDPE, YYY: density, ZZ: GMB volume %). Three particle densities (figure 1) with volume fractions (20, 40 and 60%) results in a total of nine closed cell foam types. Plasticoder plasticizes matrix resin at 160 °C into which the required amount of GMBs is added. Screw rotations in plasticoder are optimized for the minimum breakage of GMBs during processing. Earlier works do not report screw speed optimization [45]. GMB/HDPE blends as produced by plasticoder are compression molded to 165 × 165 × 3.2 mm^3 sheet by applying 5 MPa pressure at 160 °C for 10 min Molded sheets are cooled for 30 min before their removal [44]. The processing parameters

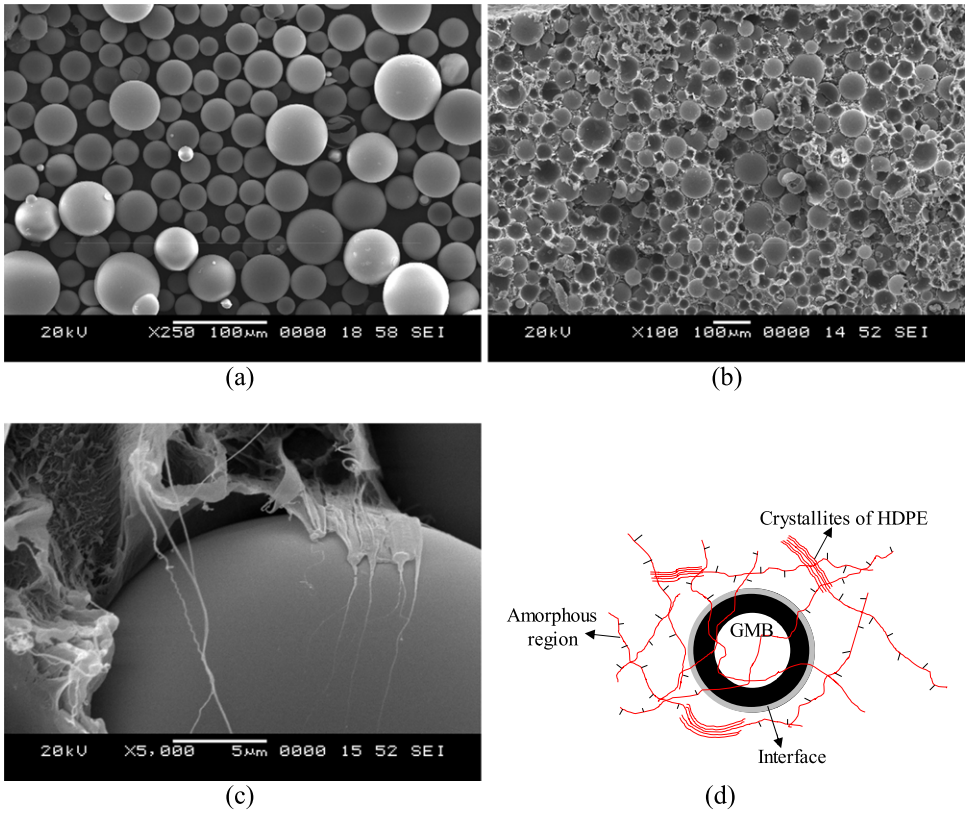

Figure 2. (a) Representative SID350 GMBs used in the present work (b) freeze-fractured micrograph of a representative H350-60 showing a uniform distribution of microballoons (c) poor interfacial bonding between the as received constituents and (d) schematic interface diagram of the constituents.

Table 1. Processing parameters utilized in the present work.

Parameters	Plasticorder	Compression molding
Mold temperature (°C)	—	160
Heating zone temperature (°C)	190	160
Screw speed (rpm)	10	—
Pressure (MPa)	—	5
Holding time (min)	5	10
Cooling time (min)	2	30
Total cycle time (min)	10	135

used are presented in table 1. Experimental (ASTM D792-13) and theoretical (rule of mixture) densities of closed cell foams vary for H200, H270 and H350 in the range of 847–608, 845–642, 853–672 (average of five replicates) and 800–500, 814–542, 830–590 kg m^{-3} respectively for 20–60 volume % GMBs in HDPE matrix. DMA 8000 (Perkin Elmer, USA) is used for DMA (dual cantilever mode, 35 mm span length, strain control configuration, and constant frequency of 1 Hz) of specimen 50 × 10 × 3 mm^3 restricting maximum displacement to 25 μm. Dynamic mechanical analysis is conducted in temperature and frequency sweep mode. Temperature is ramped from 35 to 150 °C at a rate of 5 °C min^{-1}. Melting of samples is prevented by terminating the test at 20 MPa storage modulus. In the frequency sweep testing, the temperature is stepped from 35 to 150 °C in increments of 5 °C. At each temperature step the specimen is soaked for 5 min to ensure thermal equilibrium. The dynamic properties are measured at 20 discrete frequencies logarithmically spaced between 1 and 100 Hz at each temperature step. At least five specimens of each type are tested in this phase. Due to large number of samples (three different wall thicknesses across three varying volume fractions), results of 1 and 100 Hz are presented in the manuscript. Storage modulus, loss modulus and damping factor (Tanδ) are noted for a minimum of five samples, and average values are presented for analysis. Heat of fusion, crystallinity and melting point of HDPE and their foams is carried out by Differential scanning calorimetry (DSC 6000, Perkin Elmer, USA). For each

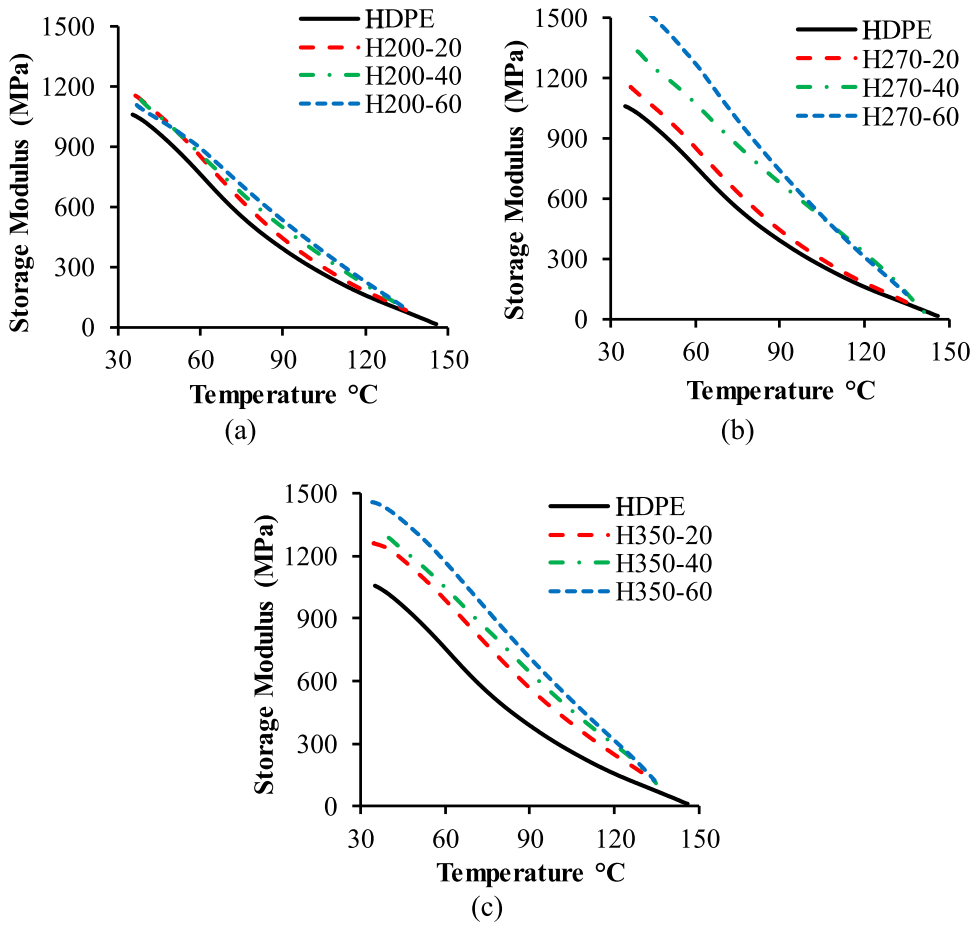

Figure 3. Storage modulus of (a) H200 (b) H270 and (c) H350 foams at 1 Hz.

measurement a sample of 5 mg is taken in hermitically sealed aluminium pan having volume of 10 μl. Test is carried out in the temperature range of 0–180 °C at a ramp rate of 10 °C min^{-1} in nitrogen atmosphere. The crystallinity of all the samples is determined using,

$$X_c = \frac{\Delta H_m}{\Delta H_m^*} \times 100 \quad (1)$$

where, ΔH_m^* is 293 J g^{-1} [46]. Micrography is carried out using JSM 6380LA, JEOL, Japan post JFC-1600 sputter coating.

Results and discussions

Representative SID350 GMBs used in the present work are presented in figure 2(a). GMB particles are spherical and have a smooth and defect-free exterior surface. Freeze-fractured micrograph of a representative H350-60 show uniform distribution of microballoons in HDPE matrix (figure 2(b)). Both the constituents, i.e. GMB and HDPE are used in as-received condition, i.e. without any surface treatment and is evident in the form of no interfacial bonding between the constituents (figure 2(c)). Figure 2(d) presents schematic interface digram [47] of the GMB/HDPE showing HDPE crystallites and amorphous regions. GMB particle breakage is inevitable as GMB reinforced HDPE closed cell foams are processed high shear mixers like plasticoders. During the fabrication of these closed cell foams, some GMB particles are fractured during blending in plasticoder [44]. Experimental densities are higher than the theoretical ones, as observed in the preceding discussion. Higher particle breakage is very obvious in the highest filler loading due to greater particle to particle interactions. The highest GMB breakage is observed in H200-60 foam. GMB failure at 60 vol. % for all the three particles (200, 270, and 350 kg m^{-3}) varies within the close range of 12.2%-17.76%. This observation signifies shear forces developed in the HDPE matrix are independent of wall thickness at higher filler loadings. Particle failure opens up the void space within the intact GMB, allowing the HDPE matrix to occupy the space along with particle debris, if any. Density reduction is not achieved as anticipated (theoretical density) owing to GMB

Table 2. Storage modulus and damping parameter of HDPE and their foams at lower and higher frequencies.

Sample type	1 Hz						100 Hz					
	50 °C		80 °C		120 °C		50 °C		80 °C		120 °C	
	E' (MPa)	$\tan\delta$ ($\times10^{-2}$)	E'at (MPa)	$\tan\delta$ ($\times10^{-2}$)	E' (MPa)	$\tan\delta$ ($\times10^{-2}$)	E' (MPa)	$\tan\delta$ ($\times10^{-2}$)	E' (MPa)	$\tan\delta$ ($\times10^{-2}$)	E' (MPa)	$\tan\delta$ ($\times10^{-2}$)
H	900.31 ± 17.98	13.60 ± 0.001	501.51 ± 10.01	18.52 ± 0.003	221.02 ± 4.40	28.13 ± 0.005	1025.52 ± 15.89	14.74 ± 0.002	591.79 ± 9.23	19.57 ± 0.001	274.21 ± 5.69	31.01 ± 0.003
H200-20	1001.08 ± 18.60	12.89 ± 0.001	581.09 ± 11.60	14.37 ± 0.002	261.15 ± 5.60	25.66 ± 0.005	1099.88 ± 16.81	15.03 ± 0.002	613.77 ± 12.47	25.98 ± 0.001	321.39 ± 4.44	33.63 ± 0.004
H200-40	1081.28 ± 19.98	13.40 ± 0.002	619.37 ± 12.40	15.22 ± 0.003	261.80 ± 5.20	26.13 ± 0.005	1295.43 ± 12.57	15.84 ± 0.002	760.73 ± 10.75	30.66 ± 0.004	380.61 ± 7.89	35.72 ± 0.005
H200-60	1081.28 ± 22.05	13.42 ± 0.003	621.34 ± 12.37	15.34 ± 0.003	294.25 ± 5.86	28.12 ± 0.005	1389.29 ± 19.24	15.97 ± 0.001	872.46 ± 12.42	33.88 ± 0.002	393.25 ± 6.32	39.02 ± 0.007
H270-20	1101.03 ± 19.96	12.86 ± 0.002	581.15 ± 11.60	14.69 ± 0.003	281.05 ± 5.60	26.63 ± 0.005	1298.31 ± 18.45	16.11 ± 0.001	957.71 ± 10.23	30.91 ± 0.001	408.13 ± 7.58	34.52 ± 0.002
H270-40	1198.04 ± 23.98	13.46 ± 0.002	881.51 ± 17.61	15.26 ± 0.002	331.46 ± 6.40	27.34 ± 0.005	1476.57 ± 24.01	17.54 ± 0.002	916.76 ± 16.74	33.67 ± 0.004	429.89 ± 6.14	36.85 ± 0.004
H270-60	1351.04 ± 27.01	14.52 ± 0.003	881.23 ± 17.60	16.50 ± 0.003	321.52 ± 6.81	28.64 ± 0.006	1498.31 ± 25.42	18.56 ± 0.001	957.71 ± 16.58	38.91 ± 0.004	458.13 ± 5.46	41.52 ± 0.003
H350-20	1181.72 ± 23.61	12.56 ± 0.002	751.06 ± 15.00	15.33 ± 0.002	281.72 ± 5.61	28.12 ± 0.006	1410.12 ± 23.12	16.95 ± 0.002	1077.47 ± 13.59	31.41 ± 0.003	428.05 ± 6.66	36.62 ± 0.004
H350-40	1204.49 ± 23.96	13.46 ± 0.004	801.50 ± 16.01	15.52 ± 0.001	339.18 ± 6.61	28.66 ± 0.006	1609.61 ± 21.75	18.25 ± 0.002	976.68 ± 15.26	34.81 ± 0.001	444.99 ± 4.58	38.88 ± 0.006
H350-60	1481.63 ± 29.61	14.73 ± 0.003	901.83 ± 18.01	17.62 ± 0.004	349.34 ± 6.96	31.52 ± 0.006	1930.05 ± 27.24	19.65 ± 0.004	1168.17 ± 17.59	39.34 ± 0.002	467.07 ± 6.58	46.05 ± 0.004

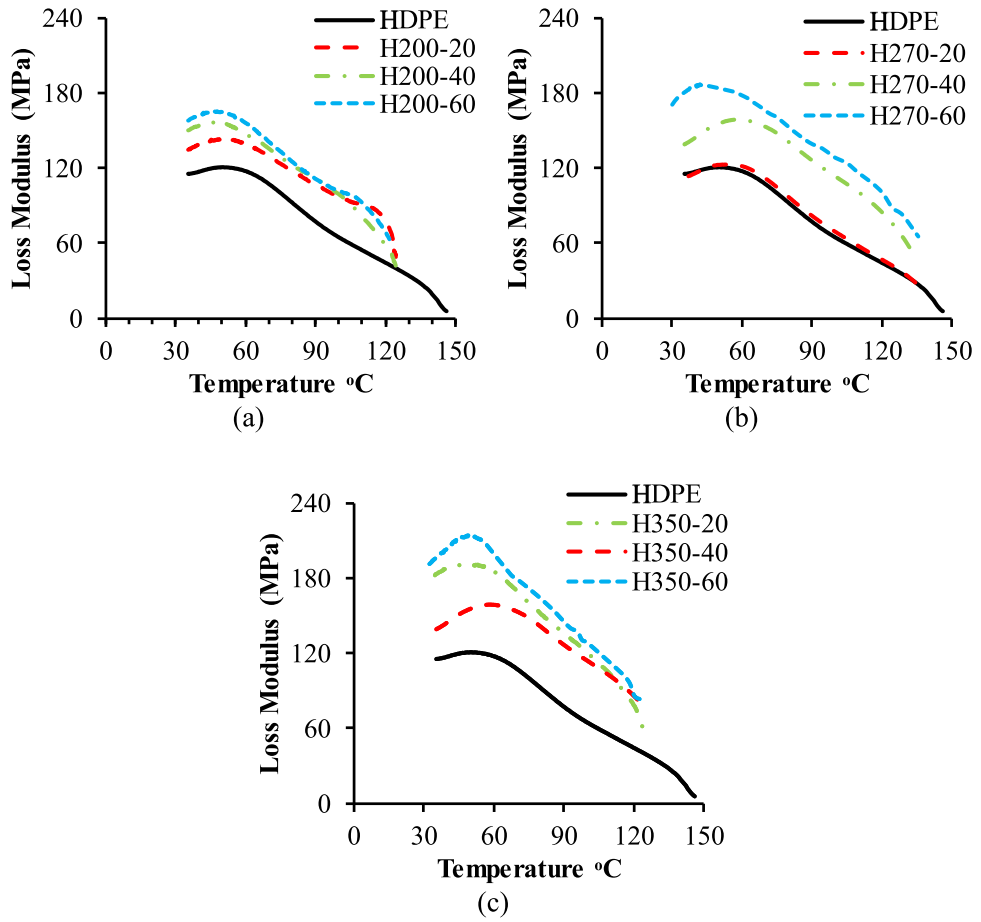

Figure 4. Loss modulus of (a) H200 (b) H270 and (c) H350 foams at 1 Hz.

breakage. Nonetheless, cheaper components can be easily realized as relatively expensive HDPE matrix is replaced by inexpensive GMB particles. Further, though GMB breakage might compromise mechanical properties, non-load bearing cheaper lightweight components can still be realized. Developed closed cell foams promise significant weight reduction (10%–36%), making them worth investigating for DMA properties.

Figure 3 shows the representative set of storage modulus for 30–150 °C temperature range. The temperature of the glass transition for HDPE is approximately -110 °C [48]. Experiments are conducted across the rubbery region. Phase transitions are not observed as step changes/peaks are absent about dynamic properties variations with temperature. Higher foam storage modulus, as compared to HDPE, is seen from figure 3 and table 2. An increase in the filler content increases storage modulus, though the difference between HYYY-40 and HYYY-60 is not significant, particularly at higher temperatures. From table 2, it can be observed that the standard deviations of these compositions overlap at the three selected reference temperatures.

The inclusion of higher modulus GMB increases the stiffness leading to higher storage modulus. The storage modulus is sensitive to the temperature. Storage modulus rise is relatively higher with increasing glass microballoon content at lower temperatures than at elevated temperatures. Thick walled GMB particle with the highest GMB content registered higher storage modulus compared to thin walled GMB foams at a lower temperature, which might be due to the higher energy absorption capabilities of thick walled microballoons. GMB content has more influence on storage modulus than wall thickness. H350-60 foam exhibits 64.64, 79.98, 58.32% and 88.20, 97.39, 70.33% rise in storage modulus respectively at 1 and 100 Hz at three reference temperatures (50, 80, and 120 °C) as compared to neat HDPE. Increasing frequency increases storage modulus for higher filler content and wall thickness. Wall thickness variations is observed to be more prominent as compared to filler content. With an increase in temperature, storage modulus decreases as matrix flows plastically beyond its softening temperature (124 °C). A significantly higher fraction of broken particles at higher particle loading may be responsible for a lack of stiffening effect. It is also observed that the closed cell foams can withstand approximately 5 °C higher temperatures before the storage modulus drops below the 20 MPa threshold.

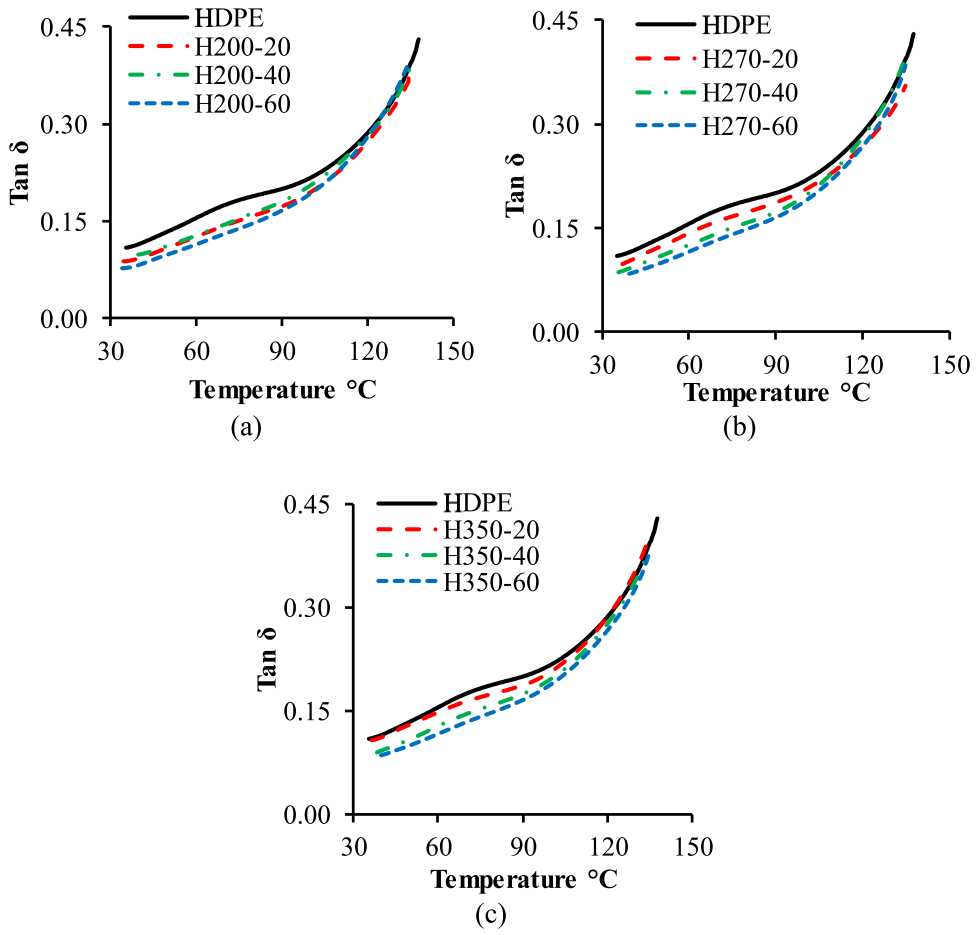

Figure 5. Tanδ of (a) H200 (b) H270 and (c) H350 foams at 1 Hz.

Loss modulus results are graphed in figure 4. As with storage modulus, the loss modulus is higher at all temperatures for foams and increases with higher particle content and wall thickness. Loss modulus is observed to be highest for H350-60 as compared to other closed cell foams (69.23%) and neat resin (80.45%). The peak found in loss modulus is at around 50 °C, corresponding to the α-relaxation in HDPE [48]. The peak appears at higher temperatures with increasing particle loading, which may indicate an increase in the crystallinity due to hollow particle infusion in compliant HDPE matrix. Hence, crystallinity estimation needs to be carried out, and results are presented in the latter part of the discussion. GMB content has a more prominent effect on loss modulus than wall thickness.

Figure 5 and table 2 presents Tanδ for the chosen temperature range at 1 and 100 Hz. Except for H350-ZZ, particularly at higher temperatures, all of the closed cell foams have lower damping parameters than the virgin HDPE at all temperatures at a lower frequency. The damping parameter of HYYY-60 foams is comparable to HDPE at all the selected temperatures. At higher frequency all the foams registered superior performance as compared to neat HDPE. Highest Tanδ is noted for H350-60 at 120 °C, i.e. below Vicat softening point (124 °C). Tanδ is less sensitive to the hollow particle content than the storage and loss moduli. The damping parameter is observed to be increasing with increasing wall thickness and GMB content. Thick wall GMB reinforced HDPE exhibited higher damping among the other foams (table 2). Tanδ is predominantly influenced by GMB content than the wall thickness variation. The developed H350-60 foams synthesized by the compression molding route is having higher storage and loss modulus coupled with higher damping. Such a foam, when deployed for structural components, results in 29.26 % weight saving and hence can be successfully used in weight-sensitive applications. Mechanical property characterization of GMB reinforced HDPE foams, as dealt in the present work, gives valuable insight for a materials designer to select the most appropriate configuration. An increase in filler content decreases the density implying promising weight-saving potential. GMB/HDPE foams achieved 36% (H200-60) weight saving in the virgin HDPE in addition to replacing the expensive matrix. These foams exhibit high stiffness to weight ratio. The inclusion of much stiffer GMBs in the HDPE matrix changes material behavior from ductile to the brittle mode [44] and can be supported by crystallinity estimations.

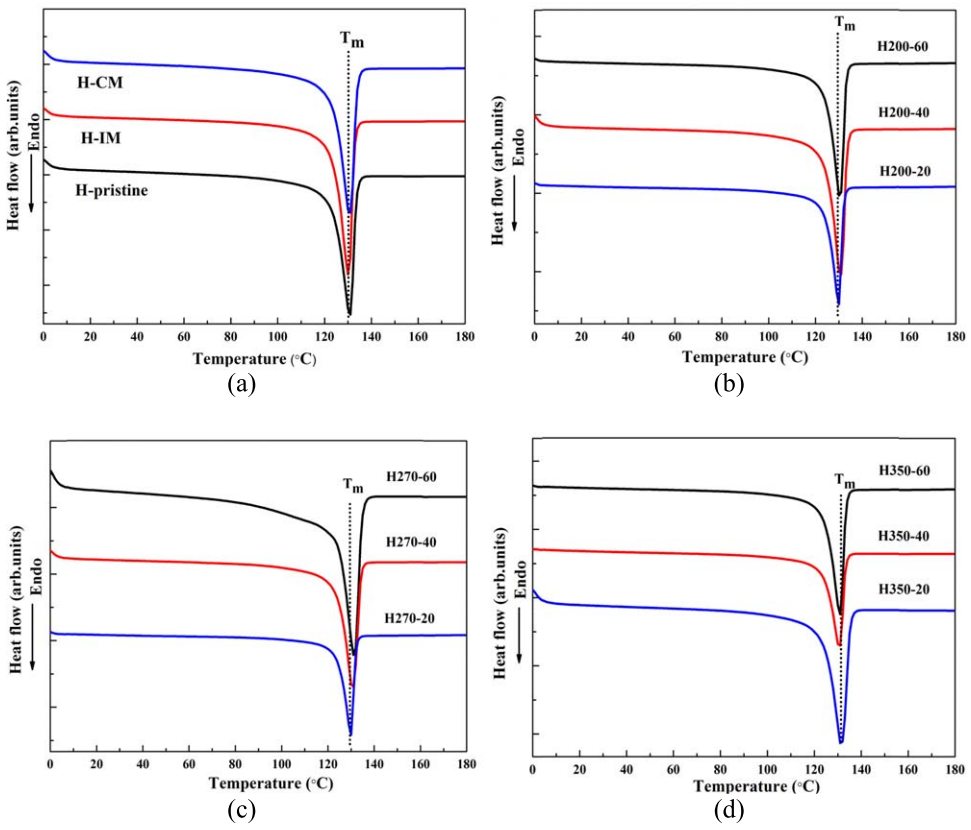

Figure 6. DSC traces of (a) HDPE (b) H200 (c) H270 and (d) H350samples.

Table 3. DSC results of HDPE and their foams.

Sample type	Melting temperature (T_m)	% crystallinity (X_c)
As received HDPE	130.4	50.4
PIM HDPE	130.4	62.5
CM HDPE	130.5	67.1
H200-20	129.9	49.9
H200-40	130.9	41.1
H200-60	131.0	32.5
H270-20	129.9	47.0
H270-40	130.8	39.7
H270-60	131.7	30.1
H350-20	131.2	44.5
H350-40	131.6	38.2
H350-60	131.8	28.1

Crystallinity measurement is carried out for as received HDPE, HDPE, and their foams using DSC analysis (figure 6). For comparative analysis, variation in crystallinity is also reported for injection molded HDPE. There is no significant change in the melting point of CM (compression molding) HDPE as compared to as received and PIM (polymer injection molding) sample (table 3). However, there is a considerable change observed in the crystallinity of PIM and CM sample compared to as-received HDPE. Melting temperature for as received HDPE is noted to be 130.4 ºC, which is slightly increased to 130.45 °C and 130.50 ºC, respectively, for PIM and CM samples. Similarly, the crystallinity of HDPE risen from 50.4 to 62.5% and 67.1% for PIM and CM samples respectively (table 3). Change in melting temperature and crystallinity indicates the rearrangement of polymer chains. It is a well-known fact that the crystallinity of HDPE varies with processing conditions such as temperature, cooling rate, etc. The melting temperature of HDPE foams gets shifted to a slightly higher temperature as compared to CM HDPE except for low density particles at lower filler contents. Besides, the $\%X_c$ of HDPE decreased with GMB

inclusion. Crystallinity decreased further with increased density and volume fraction of the fillers. This may be attributed to the fact that owing to GMB infusion in the HDPE matrix, the molecular structure of HDPE interrupts the nucleation and ordering of polymer chains during the cooling cycle of the process. Such hindering of HDPE chain mobility affects the crystallinity and HDPE crystal size [49, 50]. Filler additions have an influence over crystallinity along with processing routes utilized to synthesize such foams.

Crystallinity decreases while damping, storage, and loss modulus increased with increasing wall thickness and GMB content. As crystallinity decreases, amorphous content in the foams increases (table 3). In the amorphous phase, polymer chains do not have restrictions for their mobility thereby absorbs vibrations and relaxes. On the other hand, in crystalline phase polymer chains are tightly packed, relaxations are highly restricted. The amorphous phase plays a role in relaxation, whereas the crystalline phase takes care of rigidity. Inclusion of stiffer GMBs increases foam moduli. Further, GMBs act as an anchor to polymer chains particularly at higher filler loading compensating stiffness loss due to filler breakage. At lower filler loadings, a higher crystalline phase contributes towards DMA properties, while higher wall thickness and amorphous content influence foam with the highest GMB content. Crystallinity decreases with increasing wall thickness. This might be probably due to the availability of more glass material in the thicker spheres, which could enhance heat dissipation by the polymer chains leading to faster solidification causing lower crystallinity. The combo effect of survived particles with higher amorphous content results in the highest DMA properties in H350-60 closed cell foams making them suitable for structural components in weight-sensitive structures subjected to dynamic loadings.

Conclusions

Developed closed cell foams promise significant weight saving potential (10%–36%). Foam density reduces with increasing GMB content and increases with increasing wall thickness. Cheaper components can be realized by GMB incorporation in a relatively expensive HDPE matrix. Storage and loss modulus increases with wall thickness and GMB content. Neat HDPE registered lower storage and loss modulus as compared to foams. Thick walled GMB particle with the highest GMB content registered higher storage modulus compared to thin walled GMB foams at lower temperatures. Loss modulus is observed to be highest for H350-60 and is 80.45% higher compared to neat resin. Damping factor (Tanδ) increases with wall thickness and filler content. Tanδ is less sensitive to the hollow particle content than the storage and loss moduli. H350-60 foam registered highest Tanδ, storage, and loss modulus. Increasing stiffness due to the incorporation of stiff GMB particles leads to such an observation, which is also affirmed by crystallinity measurements. Neat HDPE sample exhibits the highest crystallinity of 67.8% as compared to all other closed cell foams. The percentage of crystallinity decreases with increasing filler content and particle wall thickness. Among foams, the lowest and highest crystallinity values are shown by H350-60 (26%) and H200-20 (51%), respectively. H350-60 closed cell foam having 29.26 % weight saving potential registered better performance as compared to other closed cell foams and neat HDPE. Such foams can be utilized for developing structural components with higher specific mechanical properties with lower carbon footprints (reduced polymer consumption).

ORCID iDs

Mrityunjay Doddamani https://orcid.org/0000-0002-5537-9404

References

[1] Jayavardhan M and Doddamani M 2018 Quasi-static compressive response of compression molded glass microballoon/HDPE syntactic foam *Composites Part B: Engineering* **149** 165–77
[2] Shutov F A 1986 Syntactic polymer foams *Chromatography/Foams/Copolymers* (*Advances in Polymer Science,* 73/74) (Berlin: Springer) pp 63–123
[3] Gupta N, Zeltmann S E, Shunmugasamy V C and Pinisetty D 2014 Applications of polymer matrix syntactic foams *JOM* **66** 245–54
[4] Grosjean F, Bouchonneau N, Choqueuse D and Sauvant-Moynot V 2009 Comprehensive analyses of syntactic foam behaviour in deepwater environment *J. Mater. Sci.* **44** 1462–8
[5] Hobaica E C and Cook S D 1968 The characteristics of syntactic foams used for buoyancy *J. Cell. Plast.* **4** 143–8
[6] Gupta N, Kishore E, Woldesenbet and Sankaran S 2001 Studies on compressive failure features in syntactic foam material *J. Mater. Sci.* **36** 4485–91
[7] Gupta N, Woldesenbet E, Hore K and Sankaran S 2002 Response of syntactic foam core sandwich structured composites to three-point bending *Journal of Sandwich Structures & Materials* **4** 249–72
[8] Licitra L, Luong D D, Strbik O M and Gupta N 2015 Dynamic properties of alumina hollow particle filled aluminum alloy A356 matrix syntactic foams *Mater. Des.* **66** 504–15
[9] Labella M, Shunmugasamy V C, Strbik O M and Gupta N 2014 Compressive and thermal characterization of syntactic foams containing hollow silicon carbide particles with porous shell *J. Appl. Polym. Sci.* **131** 40689

[10] Xie W, Yan H, Mei Q, Du M and Huang Z 2007 Compressive and fracture properties of syntactic foam filled with hollow plastic bead (HPC) *Journal of Wuhan University of Technology-Mater. Sci. Ed.* **22** 499–501
[11] Yusriah L and Mariatti M 2013 Effect of hybrid phenolic hollow microsphere and silica-filled vinyl ester composites *J. Compos. Mater.* **47** 169–82
[12] Wang L, Yang X, Zhang J, Zhang C and He L 2014 The compressive properties of expandable microspheres/epoxy foams *Composites Part B: Engineering* **56** 724–32
[13] Yung K C, Zhu B L, Yue T M and Xie C S 2009 Preparation and properties of hollow glass microsphere-filled epoxy-matrix composites *Compos. Sci. Technol.* **69** 260–4
[14] Deepthi M, Sailaja R, Sampathkumaran P, Seetharamu S and Vynatheya S 2014 High density polyethylene and silane treated silicon nitride nanocomposites using high-density polyethylene functionalized with maleate ester: mechanical, tribological and thermal properties *Materials & Design (1980-2015)* **56** 685–95
[15] Atikler U, Basalp D and Tihminlioğlu F 2006 *Mechanical and morphological properties of recycled high-density polyethylene, filled with calcium carbonate and fly ash J. Appl. Polym. Sci.* **102** 4460–7
[16] Demjen Z and Pukanszky B 1997 *Effect of surface coverage of silane treated $CaCO_3$ on the tensile properties of polypropylene composites Polym. Compos.* **18** 741–7
[17] Shah E and Rajaram 1997 *Plastic Recycling in Bangalore, India* Waste Advisers on Urban Environment and Development
[18] Farinha J, Winnik M and Hahn K 2000 Characterization of oil droplets under a polymer film by laser scanning confocal fluorescence microscopy *Langmuir* **16** 3391–400
[19] Nian G, Shan Y, Xu Q, Qu S and Yang Q 2016 Failure analysis of syntactic foams: A computational model with cohesive law and XFEM *Composites Part B: Engineering* **89** 18–26
[20] Huang R and Li P 2015 Elastic behaviour and failure mechanism in epoxy syntactic foams: The effect of glass microballoon volume fractions *Composites Part B: Engineering* **78** 401–8
[21] Tagliavia G, Porfiri M and Gupta N 2012 Influence of moisture absorption on flexural properties of syntactic foams *Composites Part B: Engineering* **43** 115–23
[22] Zeltmann. S E and B. R. Bharat Kumar N G 2016 Mrityunjay Doddamani. *Dynamic mechanical analysis of cenosphere/hdpe syntactic foams Proc. of the American Society for Composites* (Williamsburg, United States of America: DEStech Publications Inc)
[23] Shunmugasamy V C, Pinisetty D and Gupta N 2013 Viscoelastic properties of hollow glass particle filled vinyl ester matrix syntactic foams: effect of temperature and loading frequency *J. Mater. Sci.* **48** 1685–701
[24] Das A and Satapathy B K 2011 Structural, thermal, mechanical and dynamic mechanical properties of cenosphere filled polypropylene composites *Mater. Des.* **32** 1477–84
[25] Tagliavia G, Porfiri M and Gupta N 2009 Vinyl ester—glass hollow particle composites: dynamic mechanical properties at high inclusion volume fraction *J. Compos. Mater.* **43** 561–82
[26] Lin T C, Gupta N and Talalayev A 2009 Thermoanalytical characterization of epoxy matrix-glass microballoon syntactic foams *J. Mater. Sci.* **44** 1520–7
[27] Jian G, Gaohui W and Xiao Z 2009 Effect of surface-modification on the dynamic behaviors of fly ash cenospheres filled epoxy composites *Polym. Compos.* **30** 232–8
[28] Sankaran S, Sekhar K R, Raju G and Kumar M N J 2006 Characterization of epoxy syntactic foams by dynamic mechanical analysis *J. Mater. Sci.* **41** 4041–6
[29] Gupta N and Woldesenbet E 2004 Microballoon wall thickness effects on properties of syntactic foams *J. Cell. Plast.* **40** 461–80
[30] Bharath Kumar B R, Doddamani M, Zeltmann S E, Gupta N, Ramesh M R and Ramakrishna S 2016 Processing of cenosphere/HDPE syntactic foams using an industrial scale polymer injection molding machine *Mater. Des.* **92** 414–23
[31] Qiao J, Amirkhizi A V, Schaaf K and Nemat-Nasser S 2010 Dynamic Mechanical Analysis of Fly Ash Filled Polyurea Elastomer *J. Eng. Mater. Technol.* **133** 011016
[32] Saba N, Jawaid M, Alothman O Y and Paridah M T 2016 A review on dynamic mechanical properties of natural fibre reinforced polymer composites *Constr. Build. Mater.* **106** 149–59
[33] Jose S, Thomas S, Parameswaranpillai J, Aprem A S and Karger-Kocsis J 2015 Dynamic mechanical properties of immiscible polymer systems with and without compatibilizer *Polym. Test.* **44** 168–76
[34] Jones D S 1999 Dynamic mechanical analysis of polymeric systems of pharmaceutical and biomedical significance *Int. J. Pharm.* **179** 167–78
[35] Chandra R, Singh S P and Gupta K 1999 Damping studies in fiber-reinforced composites—a review *Compos. Struct.* **46** 41–51
[36] Poveda R L, Achar S and Gupta N 2014 Viscoelastic properties of carbon nanofiber reinforced multiscale syntactic foam *Composites Part B: Engineering* **58** 208–16
[37] Yang S, Taha-Tijerina J, Serrato-Diaz V, Hernandez K and Lozano K 2007 Dynamic mechanical and thermal analysis of aligned vapor grown carbon nanofiber reinforced polyethylene *Composites Part B: Engineering* **38** 228–35
[38] Yang F, Ou Y and Yu Z 1998 Polyamide 6/silica nanocomposites prepared by in situ polymerization *J. Appl. Polym. Sci.* **69** 355–61
[39] Wang X, Hu Y, Song L, Yang H, Xing W and Lu H 2011 In situ polymerization of graphene nanosheets and polyurethane with enhanced mechanical and thermal properties *J. Mater. Chem.* **21** 4222–7
[40] Lin N, Chen G, Huang J, Dufresne A and Chang P R 2009 Effects of polymer-grafted natural nanocrystals on the structure and mechanical properties of poly(lactic acid): A case of cellulose whisker-graft-polycaprolactone *J. Appl. Polym. Sci.* **113** 3417–25
[41] Kostka P, Holeczek K, Höhne R, Filippatos A and Modler N 2016 Extension and application of dynamic mechanical analysis for the estimation of spatial distribution of material properties *Polym. Test.* **52** 184–91
[42] Jia Z, Amirkhizi A V, Nantasetphong W and Nemat-Nasser S 2016 Experimentally-based relaxation modulus of polyurea and its composites *Mechanics of Time-Dependent Materials* **20** 155–74
[43] Nielsen C and Nemat-Nasser S 2015 Crack healing in cross-ply composites observed by dynamic mechanical analysis *J. Mech. Phys. Solids* **76** 193–207
[44] Jayavardhan M, Kumar B B, Doddamani M, Singh A K, Zeltmann S E and Gupta N 2017 Development of glass microballoon/HDPE syntactic foams by compression molding *Composites Part B: Engineering* **130** 119–31
[45] Deepthi M V, Sharma M, Sailaja R R N, Anantha P, Sampathkumaran P and Seetharamu S 2010 Mechanical and thermal characteristics of high density polyethylene–fly ash Cenospheres composites *Mater. Des.* **31** 2051–60
[46] Xiang D, Guo J, Kumar A, Chen B and Harkin-Jones E 2017 *Effect of processing conditions on the structure, electrical and mechanical properties of melt mixed high density polyethylene/multi-walled CNT composites in compression molding.* Materials *Testing* **59** 136–47
[47] Joshi G M, Sharma A, Tibrawala R, Arora S, Deshmukh K, Kalainathan S and Deshmukh R R 2014 Preparation and performance characterization of soft polymer composites as a function of single and mixed nano entities *Polym.-Plast. Technol. Eng.* **53** 588–95

[48] Khanna Y P, Turi E A, Taylor T J, Vickroy V V and Abbott R F 1985 Dynamic mechanical relaxations in polyethylene *Macromolecules* **18** 1302–9
[49] George G, Mahendran A and Anandhan S 2014 Use of nano-ATH as a multi-functional additive for poly (ethylene-co-vinyl acetate-co-carbon monoxide) *Polym. Bull.* **71** 2081–102
[50] Khalifa M, Mahendran A and Anandhan S 2016 Probing the synergism of halloysite nanotubes and electrospinning on crystallinity, polymorphism and piezoelectric performance of poly (vinylidene fluoride) *RSC Adv.* **6** 114052–60
[51] Doddamani M R, Kulkarni S M and Kishore 2011 Behavior of sandwich beams with functionally graded rubber core in three point bending *Polymer Composites* **32** 1541–51